KSTLE International Journal, Vol. 3, No. 2, December 2002, pp. 110-113

A Study on Lubricative Characteristics of Negative Pressure Slider

Pyung Hwang†, Sang-Shin Park and Eun-Hyo Kim*

School of Mechanical Engineering, Yeungnam University, Korea
**Department of Mechanical Engineering, Yeungnam University*

Abstract: The lubricative characteristics of negative pressure slider were performed by using coordinate transform method. Governing equation is derived by applying generalized coordinate system to the divergence formulation method. This method makes it possible to deal with an arbitrary configuration of a lubricated surface. The pressure profile of the slider is calculated. These results are compared to that from direct numerical method. The steady-state, including minimum film thickness, pitching and rolling angle are calculated by multi-dimensional Newton-Rapshon method. The stiffness and damping characteristics are also calculated.

Key words: Negative pressure slider, generalized coordinate system, divergence formulation

Introduction

Recently, a great many people in the whole world use the computers. They surf the World-Wide Web, listen to music, or see the movies and so on. The computer is adapted to various field of human life. Thus the computer industries lead modern industrial societies. One of the most important elements of the computers is hard disk drive. The higher the society is developed, the more information needs to be stored. So the capacity of hard disk needs to be higher than before.

There are several head and disks in the hard disk drive. The head are used to read and write the magnetic record on the disk. The head are flying on the disk by pressure of the air film whose thickness has sub-micron order. These air film thickness needs to be reduced in order to increase the magnetic recording capacity because the magnetic density decreased in proportion to the square of the distance between head and disk.

A Negative Pressure Sliders (NPS) were developed for this purpose. These sliders have parts on which the pressure under the ambient pressure is generated. This pressure plays a role of pulling the head near to the disk. These sliders also offer less flying height sensitivity to disk velocity, higher stiffness of the air bearing and faster take off [1] than the conventional two rail sliders. White [2] presented a design of a Transverse and Negative Pressure Contour (TPC) slider and showed the above advantages. Bogy [3] performed FDM analysis about static and dynamic characteristic of negative pressure slider, Yang [4] obtained static and dynamic characteristics from direct method and perturbed method, Kawabata [5] suggested divergence formulation (DF) method to the lubricated journal bearings.

In this work, we applied the coordinate transformation method to the negative pressure sliders who have complicate geometry. The static pressure is calculated and the steady states are found from moment equilibrium conditions. Then the stiffness and damping characteristics are calculated using the small perturbation method.

†Corresponding author: Tel: 82-53-810-2448, Fax: 82-53-813-3703
E-mail: phwang@yumail.ac.kr

Theoretical Analysis

Fundamental Equations

The arbitrary lubricated surface is considered as shown Fig. 1. (a). (s , t) is the meridian coordinate system, which is parallel to boundaries surrounding the lubricated surface. (ξ, η) is perpendicular coordinate system whose grid sizes are all 1 as shown in Fig. 1(b). The governing equations derived in the (s, t) coordinate system are transformed to the (ξ, η) coordinate system.

The mass flux $\vec{q}$ per unit length is expressed in the (s, t) coordinate system as follows;

$$\vec{q} = q^s \hat{i} + q^t \hat{j}$$

$$q^s = \frac{\rho h^3}{12\mu}\frac{\partial p}{\partial s} + \frac{1}{2}\rho h V_s \qquad (1)$$

$$q^t = \frac{\rho h^3}{12\mu}\frac{\partial p}{\partial t} + \frac{1}{2}\rho h V_t$$

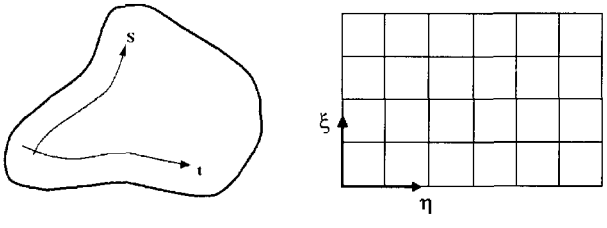

(a) (b)

Fig. 1. (a) Arbitrary surface (b) Transformed coordinate.

The unit vector $\vec{n}^{\xi}$ which is normal to the ξ = const. and $\vec{n}^{\eta}$ which is normal to the η = const. line and is directional to the increase of ξ, η respectively is expressed as,

$$\vec{n}^{\xi} = \frac{grad\xi}{|grad\xi|} = = (t_\eta \hat{i} - s_\eta \hat{j})/\sqrt{\alpha}$$
$$\vec{n}^{\eta} = \frac{grad\eta}{|grad\eta|} = = (-t_\xi \hat{i} - s_\xi \hat{j})/\sqrt{\gamma} \quad (2)$$

$\vec{n}^{\xi}$-directional mass flux component q_n^{ξ}, $\vec{n}^{\xi}$-directional mass flux component q_n^{η} is are derived respectively as

$$q_n^{\xi} = \frac{\rho}{q} \cdot \frac{\rho_\xi}{n} = (t_\eta q^s - s_\eta q^t)/\sqrt{s_\eta^2 + t_\eta^2}$$
$$q_n^{\eta} = \frac{\rho}{q} \cdot \frac{\rho_\eta}{n} = (-t_\xi q^s - s_\xi q^t)/\sqrt{s_\xi^2 + t_\xi^2} \quad (3)$$

s-t -directional pressure gradients are expressed by use of ξ, η -directional ones, as follows,

$$\frac{\partial p}{\partial s} = = (t_\eta p_\xi - t_\eta p_\xi)/J$$
$$\frac{\partial p}{\partial t} = = (s_\xi p_\eta - s_\xi p_\eta)/J \quad (4)$$

Substituting eq. (4) into eq.(1) and substituting into eq. (3), q_n^{ξ}, q_n^{η} are expressed as

$$q_n^{\xi} = \rho\{-Ap_\xi + Bp_\eta + D\}/\sqrt{\alpha}$$
$$q_n^{\eta} = \rho\{Bp_\xi - Cp_\eta + E\}/\sqrt{\gamma} \quad (5)$$

where coefficients are,

$$\alpha = s_\eta^2 + t_\eta^2 \quad \beta = s_\xi s_\eta + t_\xi t_\eta \quad \gamma = s_\xi^2 + t_\xi^2 \quad J = s_\xi t_\eta - s_\eta t_\xi$$
$$A = (h^3/(12\mu))(\alpha/J) \quad B = (h^3/(12\mu))(\beta/J)$$
$$C = (h^3/(12\mu))(\gamma/J) \quad D = (ht_\eta V_s - hs_\eta V_t)/2$$
$$E = (hs_\xi V_t - hs_\eta V_t)/2$$

In steady state , total mass flux expressed as,

$$Q_{op}^{\xi} = \int_{\eta_1}^{\eta_2} Rp_o(-A_o p_{o\xi} + B_o p_{o\eta})d\eta$$
$$Q_{oc}^{\xi} = \int_{\eta_1}^{\eta_2} Rp_o D_o d\eta$$
$$Q_{os}^{\xi} = \int_{\eta_1}^{\eta_2} R(-F_o p_{o\xi} + G_o p_{o\eta})d\eta$$
$$Q_{op}^{\eta} = \int_{\xi_1}^{\xi_2} Rp_o(B_o p_{o\xi} - C_o p_{o\eta})d\xi$$
$$Q_{oc}^{\eta} = \int_{\xi_1}^{\xi_2} Rp_o E_o d\xi$$
$$Q_{os}^{\eta} = \int_{\xi_1}^{\xi_2} R(G_o p_{o\xi} - H_o p_{o\eta})d\xi \quad (6)$$

In perturbed state, total mass flux expressed as,

$$\hat{Q}_p^{\xi} = \int_{\eta_1}^{\eta_2} R\hat{p}(-A_o p_{o\xi} + B_o p_{o\eta})d\eta +$$
$$\int_{\eta_1}^{\eta_2} Rp_o(-A_o \hat{p}_\xi + B_o \hat{p}_\eta)d\eta + \int_{\eta_1}^{\eta_2} Rp_o \hat{h}(-\hat{A}p_{o\xi} + \hat{B}p_{o\eta})d\eta$$
$$\hat{Q}_c^{\xi} = \int_{\eta_1}^{\eta_2} R\hat{p}D_o d\eta + \int_{\eta_1}^{\eta_2} Rp_o \hat{h}\hat{D}d\eta$$
$$\hat{Q}_s^{\xi} = \int_{\eta_1}^{\eta_2} R(-F_o \hat{p}_\xi + G_o \hat{p}_\eta)d\eta + \int_{\eta_1}^{\eta_2} R\hat{h}(-\hat{F}p_{o\xi} + \hat{G}p_{o\eta})d\eta$$
$$\hat{Q}_p^{\eta} = \int_{\xi_1}^{\xi_2} R\hat{p}(B_o \hat{p}_{o\xi} - C_o p_{o\eta})d\xi + \int_{\eta_1}^{\eta_2} Rp_o(B_o \hat{p}_\xi - C_o \hat{p}_\eta)d\xi +$$
$$\int_{\xi_1}^{\xi_2} Rp_o \hat{h}(\hat{B}p_{o\xi} - \hat{C}p_{o\eta})d\eta\xi$$
$$\hat{Q}_c^{\eta} = \int_{\xi_1}^{\xi_2} R\hat{p}E_o d\xi + \int_{\xi_1}^{\xi_2} Rp_o \hat{h}\hat{E}d\xi$$
$$\hat{Q}_s^{\eta} = \int_{\xi_1}^{\xi_2} R(G_o \hat{p}_\xi - H_o \hat{p}_\eta)d\xi + \int_{\xi_1}^{\xi_2} R\hat{h}(\hat{G}p_{o\xi} - \hat{H}p_{o\eta})d\xi \quad (7)$$

$$Q^{\xi} = Q_p^{\xi} + Q_c^{\xi} + Q_s^{\xi}$$
$$Q^{\eta} = Q_p^{\eta} + Q_c^{\eta} + Q_s^{\eta} \quad (8)$$

Steady-state means that supporting force by air pressure equals to the external load and moments of pitching and rolling angle about pivot point becomes zero. To obtain pitching, rolling angle and minimum film thickness at steady-state, multi-dimensional Newton Raphson method is applied.

$$f_1(h_{min}\alpha, \beta) = (F - F_o)$$
$$f_2(h_{min}\alpha, \beta) = M_y$$
$$f_3(h_{min}\alpha, \beta) = M_x$$

Geometry of air-lubricated slider bearing

Fig. 2. shows the shape and dimensions of sliders considered in this work. At this figure, (a) is the shape of conventional two-rail slider, and (b) is an example of negative pressure slider who has pocket at the center part of the slider.

Computational Results

2-rail slider

Fig. 3. shows the pressure profile from the direct method and the coordinate transformation method, respectively. The two results are similar.

The load carrying capacity versus velocity is calculated for the conventional two- rail slider in order to examine the usability of coordinate transformation method. The results are compared to that from direct method [4] and semi-implicit method [2] as shown in Fig. 4. The load carrying capacity from coordinate transformation methods are coincident with that from two other methods for the whole range of velocity within 5% errors.

Negative pressure slider

Fig. 5 shows example of negative pressure slider used in this paper. Fig. 5. (b) shows the height function of the slider and Fig. 5. (c) shows the corresponding pressure profile. The leading edge is slightly inclined and height is suddenly

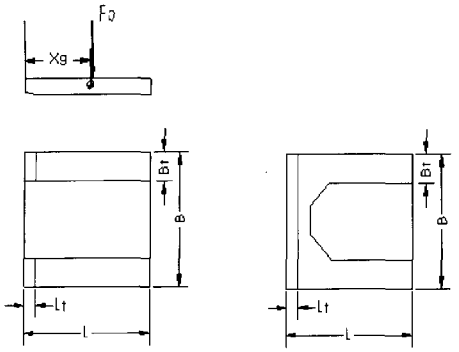

Length (L)	$4.1\times10^{-3}m$
Leading edge (Lt)	$0.71\times10^{-3}m$
Width (B)	$3.8\times10^{-3}m$
Rail width (Bt)	$0.64\times10^{-3}m$
Xg	$2.1\times10^{-3}m$
Yg	$1.05\times10^{-3}m$
External force (Fo)	$9.0\times10^{-2}(N)$
External Moment (Mx)	-1×10^{-7}
External Moment (My)	-1.5×10^{-3}
Leading Edge angle (δ)	0.83

Fig. 2. Configuration of sliders.

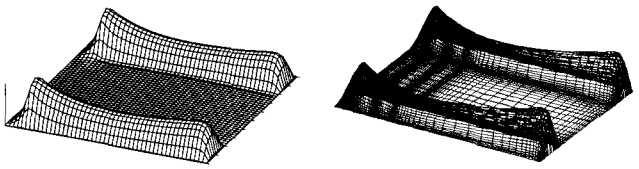

Fig. 3. Comparison between two method. (a) Direct method (b) Coordinate method.

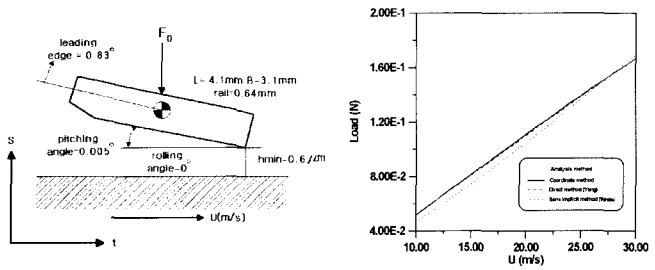

Fig. 4. Load versus velocity.

increased at the center part of the slider. This part is called the step boundary region. The positive pressure is generated from leading edge and the saddle shaped positive pressure is generated along the two-side rail. However, the negative pressure is made at the step boundary region because compressed air is expanded when they met abruptly increased height. Fig. 5. (d) shows the two-dimensional contour of this pressure profile.

Fig. 6. shows the variation of steady-state according to disk velocity . The change of minimum film thickness are presented in Fig. 6(a). The load carrying capacity is increased according to the disk velocity. This phenomenon means that the increasing rate of positive pressure at the side rail is greater

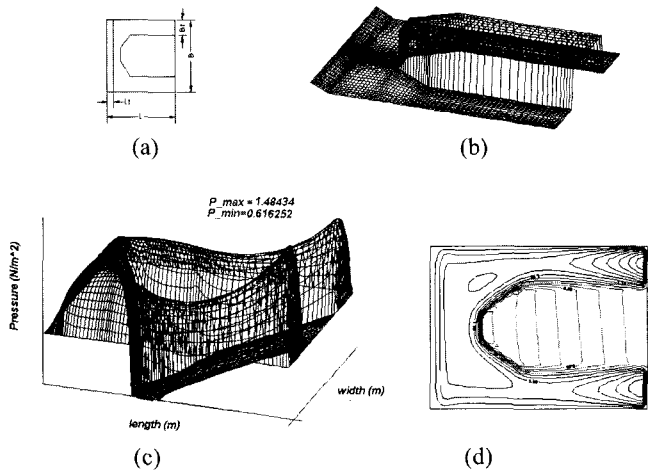

Fig. 5. An example of pressure profile for NPS. (a) geometry (b) sliders height (c) pressure distribution (d) pressure contour.

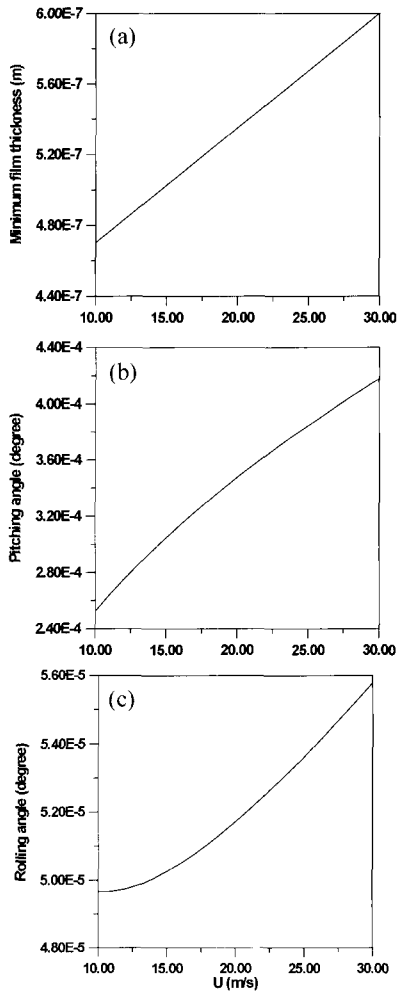

Fig. 6. Static characteristics of NPS. (a) Minimum thickness versus velocity (b) Pitching angle versus velocity (c) Rolling angle versus velocity.

than that of negative pressure. The increased load carrying capacity push the head away from the disk. As the result, the

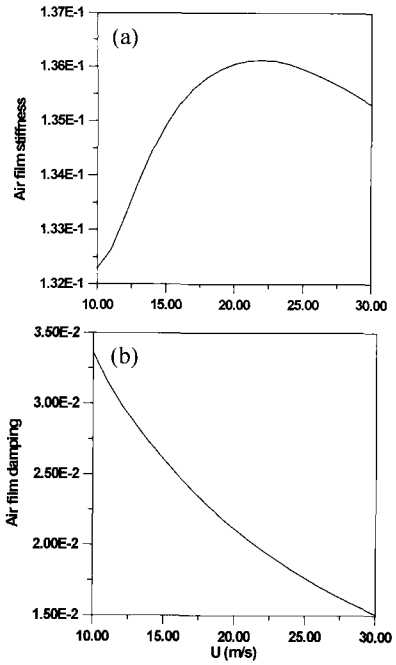

Fig. 7. Dynamic characteristics of NPS. (a) Air film stiffness versus velocity (b) Air film damping versus velocity.

minimum film thickness is increased. (b), (c) shows the variation of rolling and pitching angle versus velocity. As velocity increase, rolling and pitching angle grow linearly. This indicates that the increasing rate pressure at the leading edge is greater than any other part. The increased leading edge pressure makes the slider to be rolled slightly.

Fig. 7(a) is the graph about the influence of velocity on air bearing stiffness. When the film thickness is changed slightly, the pressure distribution is changed. The integration of pressure variation (ΔP) results in the variation of load carrying capacity (ΔF). The stiffness means that the rate of variation of load (ΔF) to the amount of change for the film thickness (Δh). In this work, stiffness coefficient can be obtained by integration of perturbed pressure calculated from eq. (7) and eq. (8). There is a specific tendency that the graph increases up to 20 m/s due to positive effect and it decreases over 20 m/s due to negative effect.

Conclusions

In this paper, a useful program is developed, which can handle the complicated geometry and compressible fluid lubrication. The coordinate transformation method is used in this program. We adapted this program to the negative pressure slider, which has ultra low film thickness. We calculated the pressure distribution for the conventional two-rail slider and compare the load carrying capacity to those from direct method and semi-implicit method. The results from the coordinate transformation method are well coincident with that of the two other methods with in 5% error. We also calculated the pressure profile of the negative pressure slider effectively by this method. The program, which is developed in this work, would be used to design the negative pressure sliders in future disk drives.

Acknowlegment

This research was supported by the Yeungnam University Research Grants in 1999.

References

1. Peng, J.-P., and Hardie, C.E., "Characteristics of Air Bearing Suction Force in Magnetic Recording Disks", ASME Journal of Tribology, Vol.118, pp. 549-554, 1996.
2. White, "Flying Characteristics of the Transverse and Negative Pressure Contour ("TNP") Slider Air Bearing", J of Tribology Vol. 119 April, pp. 241-248, 1997.
3. Miu, D.K. and Bogy D.B., "Dynamics of Gas-Lubricated Slider Bearings in Magnetic Recording Disk Files-Part:Experimental Observation", J. of Trib., Trans. ASME, Series F, Vol. 108, pp. 584-588, 1986.
4. Yang, "A study on the Lubrication Analysis of Air Lubricated Slider Bearing With Ultra Low Clearance", 1996.
5. Nobuyoshi Kawabata, "A Study on the Numerical Analysis of fluid film Lubrication by the Boundary Fitted Coordinate System [Fundamental Equation of DF method]", JSME Int, Journal, Vol. 31, No. 1, pp. 107-113, 1988.
6. Nobuyoshi Kawabata, "A Study on the Numerical Analysis of fluid film Lubrication by the Boundary Fitted Coordinate System [The case of Steady Gas Lubrication]", JSME Int, Journal, Vol. 32, No. 2, pp. 281-288, 1989.
7. Ono, K., "Dynamic Characteristics of Air-Lubricated Slider Bearing for Noncontact Magnetic Recording", J. of Lubr. Techn., Trans. ASME, Series F, Vol. 97, pp. 250-260, 1975.
8. Park, Chang, Hwang and Han, "Static Analysis of Gas Bearing with Ultra Low Clearance by the Direct Numerical Solution Method." KSME, Vol. 15, pp. 120-126, 1991.